Proc. Natl. Acad. Sci. USA
Vol. 90, pp. 7903–7907, August 1993
Neurobiology

Channel gating kinetics and synaptic efficacy: A hypothesis for expression of long-term potentiation

(paired-pulse facilitation/hippocampus/glutamate receptor model/quantal analysis)

JOSÉ AMBROS-INGERSON AND GARY LYNCH

Center for the Neurobiology of Learning and Memory, University of California, Irvine, CA 92717

Communicated by Leon N Cooper, April 8, 1993 (received for review February 8, 1993)

ABSTRACT **A kinetic model of the glutamate DL-α-amino-3-hydroxy-5-methyl-4-isoxazolepropionic acid (AMPA) receptor/channel complex was used to test whether changes in the rate constants describing channel behavior could account for various features of long-term potentiation (LTP). Starting values for the kinetic parameters were set to satisfy experimental data (e.g., affinity, mean open time, mean burst length, etc.) and physical constraints (i.e., microreversibility). The resultant model exhibited a variety of dynamic properties known to be associated with the receptor. Increasing the rate constants governing opening/closing of the channel produced an unexpected increase in the probability of the channel being open shortly after transmitter binding. This would account for the enhanced response size with LTP. Increases in rate constants produced two other aspects of LTP: (*i*) an alteration of the waveform of the synaptic response and (*ii*) an interaction with changes in desensitization kinetics. The results obtained with the model corresponded closely to those found in LTP experiments. Thus, an increase in opening/closing rates for the postsynaptic receptor channel provides a single explanation for diverse characteristics of LTP. Finally, the kinetic manipulation reduced the coefficient of variation of synaptic currents in a model involving 250 receptors. This calls into question the use of variance measures for distinguishing pre- vs. postsynaptic sites of potentiation.**

Most hypotheses about the site of change responsible for the expression of long-term potentiation (LTP) posit one of the following: (*i*) an increase in transmitter release (1); (*ii*) a change in the affinity or number of postsynaptic glutamate receptors (2); (*iii*) a decrease in the linear resistance of spines (3). Experimental studies and modeling work indicate that each of these classes of variables influences the size of synaptic currents; thus, each is a logical and biologically plausible locus for the modification underlying the potentiation effect. Changes in the kinetics of the glutamate receptor channel complex have not been proposed as the site for LTP expression, perhaps because they are not straightforwardly related to the magnitude of synaptic potentials. Yet two recent sets of observations suggest that an alteration in channel kinetics accompanies LTP. First, the decay time constant of the synaptic response, a measure known to be sensitive to the mean open time of the receptor channel (4), is reduced after induction of LTP (5); this effect is correlated with other LTP-related changes in the waveform (6). Second, aniracetam, a drug that acts selectively on the DL-α-amino-3-hydroxy-5-methyl-4-isoxazolepropionic acid (AMPA) receptor (7), has different effects on the amplitude and waveform of potentiated vs. nonpotentiated responses (8, 9). Since aniracetam modifies the kinetics of the AMPA receptor channel (10, 11), the observed interactions between drug and LTP suggest that potentiation itself changes the kinetic parameters of the channel. These findings raise the question of whether a simple alteration in one or more of the rate constants describing channel behavior could account for a significant portion of LTP phenomenology. We explore this possibility through analysis and simulation of a realistic kinetic model of the glutamate (AMPA) receptor channel.

METHODS

The kinetic model is presented in Fig. 1*A*. Realistic analysis of the properties of this model, as they relate to synaptic transmission, requires consideration of time-dependent transition rates $[k_i x_a(t); i = 1, 3]$ as transmitter concentration $x_a(t)$ changes in time. As such nonhomogeneous Poisson processes are usually mathematically intractable, our approach has been (*i*) to numerically solve the system of differential equations defined by the matrix equation $\mathbf{P}'(t) = \mathbf{R}(t)\mathbf{P}(t)$, where each entry $p_i(t)$ of the column vector $\mathbf{P}(t)$ represents the probability that the receptor is in state i (as numbered in Fig. 1*A*) at time t, and $\mathbf{R}(t)$,

$$\begin{pmatrix} -k_1 x_a(t) - k_{-4} & k_{-1} & 0 & k_{-4} & 0 \\ k_1 x_a(t) & -k_{-1} - k_d - k_o & k_r & 0 & k_c \\ 0 & k_d & -k_r - k_{-3} & k_3 x_a(t) & 0 \\ k_4 & 0 & k_{-3} & -k_3 x_a(t) - k_{-4} & 0 \\ 0 & k_o & 0 & 0 & -k_c \end{pmatrix},$$

is the transition rate matrix associated to the kinetic scheme of Fig. 1*A*, using the steady-state probabilities as initial conditions; and (*ii*) to simulate the behavior of a number of independent individual channels by generation of pseudorandom numbers with the appropriate distributions. The fifth-order Runge–Kutta method with adaptive step-size control was used to solve the system of differential equations, while the "thinning algorithm" (13) was used to generate nonhomogeneous Poisson transitions. The time course of transmitter concentration was modeled by

$$x_a(t) = \begin{cases} x_{a_b} + x_{a_o} e^{-t x_{a_r}} & \text{if } t \geq 0 \\ x_{a_b} & \text{if } t < 0, \end{cases} \quad [1]$$

where x_{a_b} and x_{a_o} are background and peak concentrations, respectively, and x_{a_r} is transmitter clearance rate.

RESULTS

The kinetic model of the AMPA receptor channel complex (Fig. 1*A*) follows that of Patneau and Mayer (14) and is similar to that proposed by Katz and Thesleff (15) to account for desensitization of the acetylcholine receptor. This is perhaps the simplest model that can account for a significant portion

The publication costs of this article were defrayed in part by page charge payment. This article must therefore be hereby marked "*advertisement*" in accordance with 18 U.S.C. §1734 solely to indicate this fact.

Abbreviations: LTP, long-term potentiation; AMPA, DL-α-amino-3-hydroxy-5-methyl-4-isoxazolepropionic acid; EPSC, excitatory postsynaptic current; CV, coefficient of variation.

of the phenomenology that has been reported for the AMPA channel such as desensitization and burst behavior (i.e., several openings closely spaced in time).

Estimation of Kinetic Parameters. Although many of the kinetic parameters of the AMPA receptor have not been measured experimentally, estimates for the model can be obtained by satisfying various physical, biochemical, and physiological properties. We proceed by listing those we have considered: (*i*) microreversibility (i.e., $k_1k_dk_{-3}k_{-4} = k_{-1}k_rk_3k_4$) should be satisfied; (*ii*) the apparent affinity K_d for L-glutamate has been estimated to be in the range 30–100 μM (16); (*iii*) mean open time of the channel ($\tau_o = 1/k_c$) is estimated to be in the range 1–3 ms; (*iv*) mean burst time (τ_b) is not much greater than τ_o; (*v*) although the association rates (k_1, k_3) for L-glutamate have not been measured for the AMPA receptor, estimates for the *N*-methyl-D-aspartate receptor are in the range 1–13 $\mu M^{-1}\cdot s^{-1}$ (17), close but not at the limit of a diffusion controlled reaction (i.e., $\approx$100 $\mu M^{-1}\cdot s^{-1}$); (*vi*) the desensitized state of the receptor is reported to exhibit higher affinity for agonist than the non-desensitized state (14, 18), hence $k_{-1}/k_1 > k_{-3}/k_3$; (*vii*) as the receptor exhibits a very fast response to a sudden increase in transmitter concentration, the state probabilities, when in the steady state with a low background concentration of agonist, must favor the unbound sensitized over the unbound desensitized state; (*viii*) shut time distributions in single-channel experiments with a constant concentration of agonist exhibit a significant component of short events (0.3–0.6 ms) plus two longer ones (4–30 and 70–400 ms) (11, 19). A significant and much shorter component ($\approx$0.05 ms) has been observed in cultured granule cells from rat cerebellum (19).

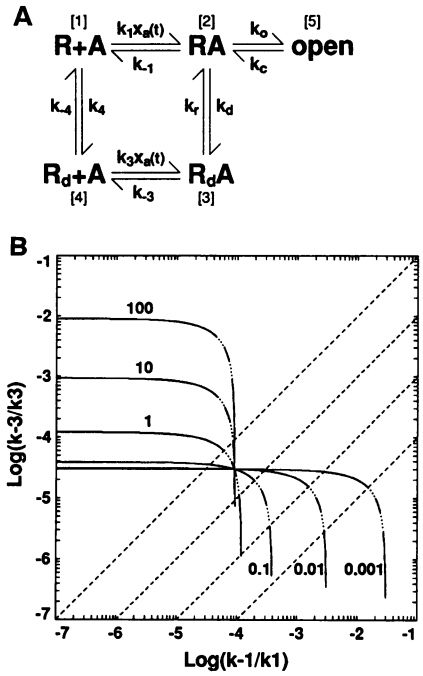

FIG. 1. Kinetic model of AMPA receptor channel complex and relationships between the ratio of rate constants for an affinity of 30 μM. (*A*) Five-state cyclic model where A represents agonist and open represents conducting state of the channel, while the remaining nonconducting states, R and R_d, are unbound sensitized and desensitized states, respectively, and RA and R_dA are ligand-bound counterparts. Accordingly, k_1 and k_{-1} are association and dissociation rates for sensitized states, k_3 and k_{-3} are rates for desensitized states, k_d and k_r are desensitization and resensitization rates of ligand-bound states, k_4 and k_{-4} are rates for unbound states, and k_o and k_c are opening and closing rates. (*B*) Logarithmic plot of ratio of dissociation/association rates of sensitized states (*x* axis) and that of desensitized states (*y* axis) for a K_d of 30 μM for the model in *A* based on Eq. 2, where k_c/k_o ratio = 0.5. Each curve corresponds to a particular value of k_r/k_d ratio as indicated by the attached number. Solid/dotted line segments on each curve correspond to ranges of values of P_R, the proportion of receptors in the unbound sensitized state in the steady state for a negligible concentration of agonist (see Eq. 3). Left to right: $P_R \leq 0.5$; $0.5 < P_R \leq 2/3$; $2/3 < P_R \leq 0.8$; $0.8 < P_R \leq 0.9$; $0.9 < P_R$. Dashed diagonal lines correspond to constant values of the ratio of the affinities of sensitized to desensitized states. Left to right: 1, 10, 100, and 1000.

Assuming that microreversibility is satisfied, the K_d for the model in Fig. 1*A* is obtained by derivation of the steady-state probabilities and is given by

$$K_d = \left(\frac{k_{-1}}{k_1} + \frac{k_d}{k_r}\frac{k_{-3}}{k_3}\right)\left(1 + \frac{k_d}{k_r} + \frac{k_o}{k_c}\right)^{-1}, \quad [2]$$

which depends only on the ratio of the rates between states and not on the individual values. Similarly, P_R, the steady-state proportion of channels in the unbound sensitized state (for a negligible concentration of agonist) is given by

$$P_R = \left(1 + \frac{k_4}{k_{-4}}\right)^{-1}. \quad [3]$$

Mean burst time, τ_b, is also readily obtained and is given by

$$\tau_b = \tau_o\left(1 + \frac{k_o}{k_d + k_{-1}}\right) + \tau_{bc}\left(\frac{k_o}{k_d + k_{-1}}\right), \quad [4]$$

where τ_{bc}, the mean closed time within a burst, is given by

$$\tau_{bc} = \frac{1}{k_{-1} + k_d + k_o}, \quad [5]$$

while P_{bc}, the proportion of shut intervals generated by an open $\rightarrow$ RA $\rightarrow$ open transition, is

$$P_{bc} = k_o\tau_{bc}. \quad [6]$$

Examination of Eq. 2 reveals that a decrease in closing rate k_c (i.e., increasing mean open time) would increase affinity (reduce K_d value), whereas a decrease in desensitization rate k_d would decrease it (provided $k_{-1}/k_1 \cdot k_3/k_{-3} > 1 + k_o/k_c$). Eq. 2 allows us to map the relationships between the ratio of the rate constants for a given K_d. Fig. 1*B* shows the results obtained when K_d = 30 μM and k_c/k_o = 0.5 (i.e., mean open time is twice the mean time to open) for a range of values of k_r/k_d. Similar results are obtained for a range of values of K_d and k_c/k_o (data not shown). Solid/dotted line segments indicate ranges of values of P_R along the curve. Consideration of the curves in Fig. 1*B* in light of point *vi* above (i.e., that $k_{-1}/k_1 > k_{-3}/k_3$) indicates that $k_r/k_d < 1$ as the required value should lie to the right of the diagonal. Stability considerations further suggest that $k_r/k_d \ll 1$ (i.e., resensitization is much slower than desensitization). On the other hand, examination of the P_R values in light of point *vii* above indicates that k_r/k_d is not likely to be <0.01 if the ratio of the affinities for the sensitized to the desensitized states is to remain not much larger than 100.

The kinetic parameters used as controls in the following simulations are listed in Fig. 2 legend. All of the above points are satisfied by the values chosen. The response of the model to a sudden increase in concentration (4 mM for 100 ms) is shown in Fig. 2*A*. Note the fast peak response and subsequent desensitization. Shut time distribution obtained from a simulation of a single channel at a constant concentration of agonist for 10 min is shown in Fig. 2*B*. The distribution is fitted by the sum of three exponentials with time constants and relative areas (in parentheses) of 0.38 (34%), 15 (16%), and 120 (50%) ms, results that agree reasonably well with

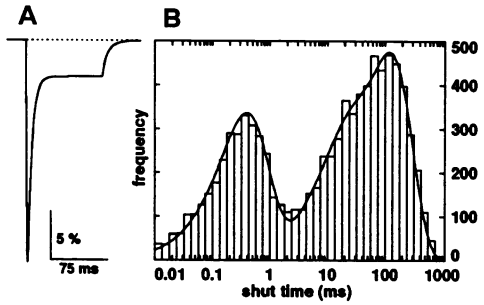

FIG. 2. Response of the model to a pulse of agonist and distribution of shut times for a constant concentration of agonist. (*A*) Probability that receptor is in open state at time t for a sudden increase in agonist concentration (from 0.1 μM to 4 mM for 100 ms and back to 0.1 μM) for steady-state probabilities as initial conditions. Peak response was 23%, whereas steady-state response during the pulse was 3.7%. Kinetic parameters were set as follows: $k_1 = 1$ $\mu M^{-1}s^{-1}$, $k_{-1} = 1/1$ ms^{-1}, $k_3 = 10$ $\mu M^{-1}s^{-1}$, $k_{-3} = 1/9.97$ ms^{-1}, $k_d = 1/1.36$ ms^{-1}, $k_r = 1/61$ ms^{-1}, $k_4 = 1/1000$ ms^{-1}, $k_{-4} = 1/450$ ms^{-1}, $k_o = 1/1.1$ ms^{-1}, $k_c = 1/2$ ms^{-1}. From these values we obtain the following (see Eqs. 2–6): $K_d = 30.42$ μM, $P_R = 69\%$, $\tau_b = 3.25$ ms, $\tau_{bc} = 0.38$ ms, $P_{bc} = 34.38\%$. (*B*) Frequency distribution of shut times for simulation of a single channel at a constant concentration (100 μM) of agonist for 10 min. Distribution is shown fitted by the sum of three exponentials with time constants and relative areas (in parentheses) of 0.38 (34%), 15 (16%), and 120 (50%) ms. Note agreement between values of the short shut time component and those predicted by τ_{bc} and P_{bc}.

those that have been reported: e.g., 0.4 (33%), 4.2 (18%), and 71 (49%) ms (11).

Of particular importance are the estimates for k_{-1}, k_d, and k_o. Simultaneous satisfaction of the two following points indicates that the estimated values for k_o and $k_{-1} + k_d$ are adequate: (*i*) the predicted mean intraburst shut time τ_{bc} (see Eq. 5) for the model parameters agrees with the observed mean short closed time component; and (*ii*) the proportion of reported short shut times is in reasonable agreement with that predicted by P_{bc} (see Eq. 6).

Increasing the Opening/Closing Rates Reproduces Diverse Features of LTP. The effects of increasing the rate constants for channel opening and closing (k_o, k_c) are shown in Fig. 3*A* (*Inset*). The striking result of this was to increase both the slope and amplitude of the synaptic current by ≈60%, indicating that a facilitation comparable in amplitude to LTP can be obtained by a simple change in open/close rates of the glutamate receptor channel. Previous studies with "disinhibited slices," slices in which inhibitory currents were blocked and postsynaptic cell discharges were suppressed, established that LTP is associated with a decrease in the decay time constant (decay τ) of synaptic responses (5); subsequent work confirmed this and showed that a correlated reduction in rise time occurs as well (6). The effects were on the order of 0.20 and 0.37 ms (5–10%) for the rise time and decay τ, respectively. Waveform alterations of these magnitudes also occurred in the model after changing the rate constants. The waveform distortions are evident in Fig. 3*A*, where the responses obtained before and after changing the rate constants are normalized for amplitude and superimposed. Note that the $t.9$ rise time value (i.e., time required to reach 90% of peak amplitude) is reduced by 0.29 ms and that the decay τ is also substantially decreased by 0.35 ms. These effects are robust in the sense that they are reproduced qualitatively across a range of parameter settings for the model and are not dependent on the assumption that desensitization is associated with high affinity.

Fig. 3*B* (*Inset*) shows the synaptic currents generated by the model in response to two concentrations of transmitter, while Fig. 3*B* shows the two responses normalized for amplitude and superimposed. The waveforms are not notice-

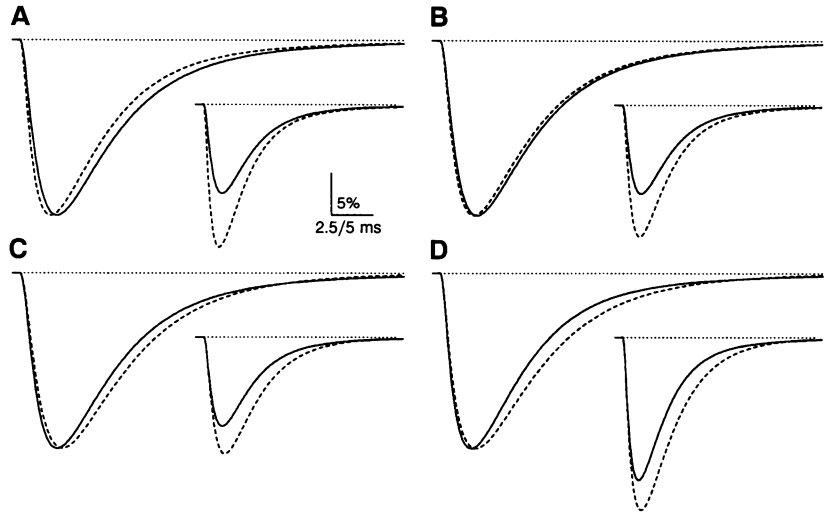

FIG. 3. Effects of changing rate constants and initial agonist concentration on responses produced by the model when agonist concentration is modeled as a sharp increase that decays exponentially thereafter. (*Insets*) Traces indicate probability that receptor is in open state at time t for control (solid line) and experimental (dashed line) conditions. Large traces correspond to those in *Insets* but are normalized for peak amplitude to better appreciate waveform alterations. Eq. 1 was used to model the time course of agonist concentration. In all control responses, background concentration was $x_{a_b} = 1$ μM, and peak concentration was $x_{a_o} = 1000$ μM with a clearance rate of $x_{a_r} = 1/1.25$ ms^{-1}, which is somewhat slower than that deduced from diffusion calculations (20) but is in accord with recent experimental estimates for the synaptic cleft (21). Unless indicated otherwise, kinetic parameters of the control response are those listed in Fig. 2 legend. Control response so obtained had a peak amplitude of 10.3%, a decay τ of 4.43 ms, and a $t.9$ rise time of 1.41 ms. (*A*) Opening and closing rates were increased to $k_o = 1/0.35$ and $k_c = 1/0.96$ ms^{-1}. Peak amplitude increased by 60.5%, while decay τ and $t.9$ changed by $\Delta\tau = -0.35$ and $\Delta t.9 = -0.29$ ms. (*B*) Initial concentration of agonist was increased to $x_{a_o} = 2000$ μM. Peak amplitude increased by 48.4% where $\Delta\tau = -0.03$ and $\Delta t.9 = -0.16$ ms. (*C*) Desensitization and resensitization rates were decreased to $k_d = 1/6.8$ and $k_r = 1/290$ ms^{-1}, which resulted in an increase in k_{-3} to 1/9.48 ms^{-1} to satisfy microreversibility and a reduction in apparent affinity to $K_d = 31.9$ μM. Peak amplitude increased by 31%, where $\Delta\tau = 0.38$ and $\Delta t.9 = 0.20$ ms. (*D*) Decreasing desensitization/resensitization rates after increasing opening/closing rates. Control response is the experimental response in *A* from which desensitization and resensitization rates were decreased as in *C* to obtain experimental trace parameters. Peak amplitude increased by 20.9%, where $\Delta\tau = 0.74$ and $\Delta t.9 = 0.14$ ms.

ably different, as evidenced by their similar values for the decay time constants. However, the response to the higher concentration is shifted slightly to the left; this is detected as a 0.16-ms decrease in the rise time measure $t.9$. Experiments using disinhibited slices have obtained effects very similar to those described in Fig. 3*B*. Paired-pulse facilitation was used in those studies to transiently increase release in the Schaffer-commissural projections to field CA1. This resulted in an ≈50% increase in the amplitude of the field excitatory postsynaptic potential with no detectable change in the decay τ (5) but a noticeable (average, 0.18 ms) leftward shift of the response (6). Moreover, increased transmitter concentration in the simulation produced the same increases in amplitude in the control and potentiated responses in Fig. 3*A* (results not shown). Thus, the absence of marked interactions between release and LTP found in experiments was also obtained in the model (22, 23).

Interactions Between Aniracetam and LTP Are Reproduced by the Model. The nootropic drug aniracetam has a potent and selective effect on the behavior of the glutamate receptor channel (7). It prolongs the time the channels remain open in the presence of agonists (10, 11) and causes a similar increase in the duration of synaptic responses in hippocampal slices (7, 8) and cultured cells (10). Three lines of evidence suggest that these effects are due to a slowing of desensitization. First, the response to kainic acid at concentrations that bind the AMPA receptor is unaffected by aniracetam (7); this agonist does not induce desensitization of the receptor (14). Second, aniracetam causes a small (5–10%) but reliable decrease in agonist binding to the AMPA receptor (24); this is as expected for a drug that slows the conversion of the receptor to a high-affinity, desensitized state (see Eq. 2). Third, single-channel analysis suggests that the major effect of aniracetam is to increase the duration of bursts of openings, with lesser changes in the mean open time of the channel (11).

Accordingly, the effects of aniracetam were represented in the model as a decrease in the desensitization/resensitization rate constants (k_d, k_r) within the range of the experimental values obtained by Vyklicky *et al.* (11). Fig. 3*C* (*Inset*) shows the effect of this. Note that the amplitude of the response is increased by ≈30%, which corresponds to the change obtained in physiological experiments (7, 8). Comparison of normalized responses before and after the decrease in rate constants (Fig. 3*C*) shows that the experimental currents have an increased rise time and a still greater increase in decay time constant. Both changes are comparable in magnitude to those found in experiments with *in vitro* hippocampal slices (5, 10).

Aniracetam causes a smaller increase in the amplitude of potentiated vs. nonpotentiated responses (8, 9, 24). It also has different effects on the waveform of the response after induction of LTP (ref. 9; A. Kolta, J.A.-I., J. Larson, and G.L., unpublished data). Tests for interactions between aniracetam and LTP were made in the present model by combining the increases described above in the opening/closing rates (LTP) with decreases in the rates of desensitization/resensitization (aniracetam). The results are shown in Fig. 3*D* (*Inset*). As illustrated, the "drug" increased the amplitude of the response to a lesser degree after than before LTP (compare Fig. 3 *C* and *D Insets*). The degree to which aniracetam had a smaller effect on the amplitude of the potentiated vs. control response is very similar to that obtained experimentally. Thus, the same change in rate constants that yields a LTP-like effect combined with a decrease in the rate of desensitization reproduces an interaction of LTP with aniracetam. The similarity between model and experimental results extends to the interactions between LTP and aniracetam on the waveform of synaptic responses. Fig. 3*D* shows the normalized superimposed responses for the LTP vs. LTP + aniracetam conditions. Note that the effect of the drug on the rise time is slightly smaller after LTP while its action on the decay time constant is larger (compare Fig. 3 *C* and *D*). This pattern agrees well with that obtained in physiological experiments with disinhibited slices (A. Kolta, J.A.-I., J. Larson, and G.L., unpublished data).

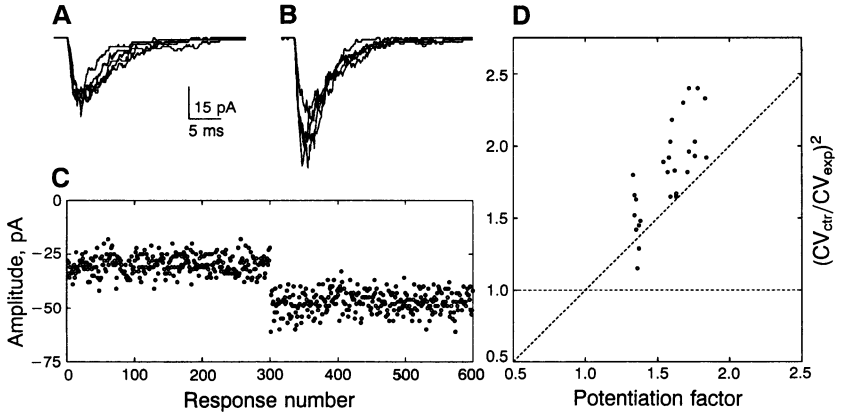

FIG. 4. Variance analysis of proposed mechanism of LTP expression. (*A*) Sample of five control EPSCs generated by simulation of 250 independent receptors, each with a conductance of 12.5 pS at a holding potential of −80 mV using kinetic parameters of the control trace of Fig. 3*A*. Time course of agonist concentration was modeled as in, and with same values of, the control traces of Fig. 3—i.e., as a sharp increase that decreases exponentially thereafter. Each trace represents the sum of currents generated by receptors in the open state, where the initial state was selected from steady-state probabilities distribution. (*B*) Sample of five EPSCs when opening/closing rates were increased as in the experimental trace of Fig. 3*A*. (*C*) Plot of amplitudes of simulated EPSCs before and after increasing the opening/closing rates as indicated in *A* and *B*; 300 independent traces were generated for each condition. Amplitude of the control traces was −29.9 ± 4.35 pA, while that of the experimental traces was −47.2 ± 4.99 pA ($\bar{x}$ ± SD), which corresponds to a potentiation factor of 1.58 with a squared CV of $(CV_{ctr}/CV_{exp})^2 = 1.89$. (*D*) Plot of results from 27 experiments performed as described in *C*. CV was obtained for amplitudes of each condition and is plotted as $(CV_{ctr}/CV_{exp})^2$ on the *y* axis as a function of the mean degree of potentiation (*x* axis). The 27 cases were obtained from nine control conditions, all sharing the same kinetic parameters as the control trace in Fig. 3*A*, but with different initial agonist concentration and clearance rates; for each of these, opening/closing rates were increased to 3 different degrees, leaving everything else unchanged. The nine conditions of initial concentration and clearance rate of transmitter were obtained as all possible combinations of 500, 1000, and 2000 μM for x_{a_0} and 1/0.75, 1/1.25, and 1/1.75 ms^{-1} for x_{a_τ} (see Eq. 1). The three degrees of potentiation were obtained by increasing opening/closing rates as follows: $k_o = 1/0.55$ and $k_c = 1/1.27$, $k_o = 1/0.35$ and $k_c = 1/0.96$, and $k_o = 1/0.25$ and $k_c = 1/0.76$ ms^{-1}, which produced increases in amplitude of ≈36%, ≈60%, and ≈76%, respectively.

Coefficient of Variation (CV) of Synaptic Responses Is Affected by Changes in Rates of Opening/Closing. It has been reported that LTP reduces the CV of synaptic responses in field CA1 of the slice (25, 26). While this finding is controversial (see ref. 27), it was of interest to test whether modifications in the rates of opening/closing have any consequences for response variance. To do this, 250 receptors (each of conductance 12.5 pS) were simulated before and after an increase in the opening/closing rates. Fig. 4 *A* and *B* shows a collection of individual excitatory postsynaptic currents (EPSCs) generated by the simulation before and after increasing the opening/closing rates, respectively, using the kinetic parameters of the corresponding traces in Fig. 3*A*. Note that the responses exhibit a considerable degree of variability despite the presence of the same time course and concentration of transmitter; this reflects the probabilistic nature of postsynaptic events. Experiments were done with 300 EPSCs collected before and 300 collected after increasing the opening/closing rate constants (i.e., pre- and post-LTP). Fig. 4*C* shows the amplitudes obtained in one experiment. CV was calculated for the two conditions; this was repeated for 27 experiments in which the percentage change in opening/closing mean times was varied between 55% and 80% to obtain three degrees of potentiation, and initial concentration and clearance rates of the transmitter were varied 4-fold. Fig. 4*D* summarizes the results in a manner used in the above noted papers; i.e., the ratio of CVs squared $(CV_{ctr}/CV_{exp})^2$ is plotted as a function of mean increase in amplitude. As shown, the normalized variance of the response is reduced after LTP and the magnitude of the effect scales with the degree of potentiation. This result closely approximates that reported by Bekkers and Stevens (25).

DISCUSSION

The results demonstrate that a diverse array of LTP phenomenology can be approximated with reasonable accuracy in a model of the glutamate receptor by a simple increase in the channel's opening/closing rate constants. While the decrease in rise time and decay time constant of the synaptic currents produced by this manipulation make intuitive sense, the sensitivity of response amplitude to those rate constants was unexpected. The relative changes in response amplitude vs. waveform parameters produced by the increase in kinetic parameters agree well with the alterations obtained following induction of LTP in disinhibited slices; i.e., a much larger change in amplitude relative to alterations in waveform (see refs. 5 and 6).

Aniracetam has different effects on amplitude and waveforms of potentiated vs. control synaptic responses; these effects provide strong constraints on any hypothesis regarding LTP expression. Slowing desensitization kinetics in the present model reproduced the effects of aniracetam on the amplitude and waveform of synaptic responses. The simulated drug effect caused a smaller increase in amplitude of potentiated vs. control responses with a lesser effect on the $t.9$ rise time and a greater effect on decay τ. This is the pattern obtained in physiological studies.

Finally, the simulations showed that the probabilistic nature of channel events results in a significant variability of EPSCs (i.e., postsynaptic variance) and that the normalized variance of a population of channel responses is reduced by increasing the opening/closing rate constants. This result is of interest because of reports that LTP in field CA1 is associated with an effect of this kind (25, 26) and because it questions the utility of variance analysis as a tool to discriminate between pre- and postsynaptic variables responsible for alterations in synaptic efficacy. Whether the effects obtained in the simulation would be detectable against the background of variability in release and in a multisynaptic situation as is found in physiological experiments is not known. In any event, the change in rate constants used to produce LTP in the model does accurately reproduce an aspect of LTP reported in the literature.

Hence, a single mechanism in the model—an increase in the rates of opening/closing of the channel—accounts for a diverse array of experimental observations related to LTP expression. Preliminary analysis indicates that one of the main factors responsible for enhancing response size is a marked increase in the probability of initiating (or continuing) a burst when the opening rate is increased (see Eq. 6).

It should be noted that the hypothesis that LTP is due to an increase in the rate constants for opening/closing of the glutamate receptor channel does not rule out contributions from changes in receptor affinity or channel conductance (12). Changes in these variables would probably scale the amplitude increases obtained by kinetic changes alone. However, as shown above, the single change in opening/closing rates is adequate for a LTP effect of the magnitude typically reported. The essential experimental question raised by this hypothesis concerns the existence of a modifiable agent in the synaptic environment, which selectively affects channel kinetics as described above. The extreme persistence of LTP further constrains the nature of this variable; i.e., it would need to be related to a very stable aspect of the synapse.

We thank Rafael Saavedra-Barrera and Arlette Kolta for helpful discussions and Jackie Porter and Marla Lay for secretarial assistance. This work was supported by the Air Force Office of Scientific Research Grant 89-0383.

1. Bliss, T. V. P. & Lynch, M. A. (1988) in *Long-Term Potentiation: From Biophysics to Behavior*, eds. Landfield, P. W. & Deadwyler, S. A. (Liss, New York), pp. 3–72.
2. Lynch, G. & Baudry, M. (1984) *Science* **224**, 1057–1063.
3. Rall, W. (1978) in *Studies in Neurophysiology*, ed. Porter, R. (Cambridge, Univ. Press, Cambridge, MA), pp. 203–209.
4. Magleby, K. L. & Stevens, C. F. (1972) *J. Physiol. (London)* **223**, 173–197.
5. Ambros-Ingerson, J., Larson, J., Xiao, P. & Lynch, G. (1991) *Synapse* **9**, 314–316.
6. Ambros-Ingerson, J., Xiao, P., Larson, J. & Lynch, G. (1993) *Brain Res.* **620**, 237–244.
7. Ito, I., Tanabe, S., Khoda, A. & Sugiyama, H. (1990) *J. Physiol. (London)* **424**, 533–543.
8. Staubli, U., Kessler, M. & Lynch, G. (1990) *Psychobiology* **18**, 377–381.
9. Staubli, U., Ambros-Ingerson, J. & Lynch, G. (1992) *Hippocampus* **2**, 49–58.
10. Tang, C.-M., Shi, Q.-Y., Katchman, A. & Lynch, G. (1991) *Science* **254**, 288–290.
11. Vyklicky, L., Jr., Patneau, D. K. & Mayer, M. L. (1991) *Neuron* **7**, 971–984.
12. Shahi, K. & Baudry, M. (1992) *Proc. Natl. Acad. Sci. USA* **89**, 6881–6885.
13. Ross, S. M. (1989) *Introduction to Probability Models* (Academic, San Diego), 4th Ed.
14. Patneau, D. K. & Mayer, M. L. (1991) *Neuron* **6**, 785–798.
15. Katz, B. & Thesleff, S. (1957) *J. Physiol. (London)* **138**, 63–80.
16. Honoré, T., Drejer, J., Nielsen, E. O. & Nielsen, M. (1989) *Biochem. Pharmacol.* **38**, 3207–3212.
17. Benbeniste, M. & Mayer, M. L. (1991) *Biophys. J.* **59**, 560–573.
18. Trussel, L. O. & Fischbach, G. D. (1989) *Neuron* **3**, 209–218.
19. Howe, J. R., Colquhoun, D. & Cull-Candy, S. G. (1988) *Proc. R. Soc. Lond. B* **233**, 407–422.
20. Eccles, J. C. & Jaeger, J. C. (1958) *Proc. R. Soc. Lond. B* **148**, 38–56.
21. Clements, J. D., Lester, R. A., Tong, G., Jahr, C. E. & Westbrook, G. L. (1992) *Science* **258**, 1498–1501.
22. Muller, D. & Lynch, G. (1989) *Brain Res.* **479**, 290–299.
23. Zalutsky, R. A. & Nicoll, R. A. (1990) *Science* **248**, 1619–1624.
24. Xiao, P., Staubli, U., Kessler, M. & Lynch, G. (1991) *Hippocampus* **1**, 373–390.
25. Bekkers, J. M. & Stevens, C. F. (1990) *Nature (London)* **346**, 724–729.
26. Malinow, R. & Tsien, R. W. (1990) *Nature (London)* **346**, 177–180.
27. Foster, T. C. & McNaughton, B. L. (1991) *Hippocampus* **1**, 79–91.